BeFORECAST

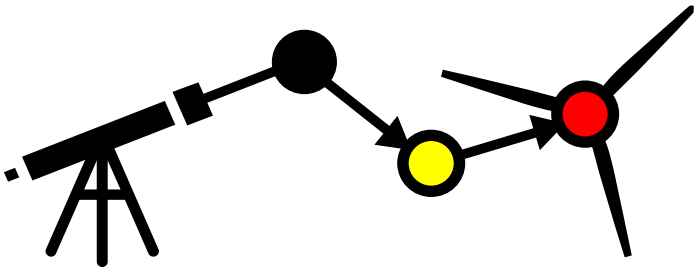

Deliverable: Overview of BeFORECAST field and virtual measurement campaigns

Deliverable No.: D1.1

economie
FOD Economie, K.M.O., Middenstand en Energie

This project has received funding from the Energy Transition Fund of the Belgian Federal Public Service for Economy, SMEs, and Energy (FOD Economie, KMO, Middenstand en Energie)

DOCUMENT CONTROL SHEET

DOCUMENT INFORMATION	
Document title	Overview of BeFORECAST field and virtual measurement campaigns
Author(s), (organization)	Wim Munters (VKI) Gertjan Glabeke (VKI) Pieter-Jan Daems (VUB) Geert Smet (RMI) Laurent Delobbe (RMI) Johan Meyers (KU Leuven)
Deliverable No.	D1.1
Work Package No.	WP1
Lead beneficiary	VKI
Dissemination level	Public
Date of issue	31/10/2025

DOCUMENT APPROVAL	
Date	Approver
31/10/2025	Wim Munters
Date	WP leader
31/10/2025	Wim Munters
Date	Coordinator
31/10/2025	Wim Munters

DOCUMENT SUMMARY

This deliverable provides an overview of the BeFORECAST field and virtual measurement campaigns carried out in the Belgian North Sea. These campaigns aim to overcome the scarcity of offshore observations by deploying nacelle-mounted LiDARs in existing wind farms, installing a LiDAR and ultrasonic anemometer on the Westhinder (MP7) platform near the future Princess Elisabeth Zone, and assessing the suitability of weather radars for offshore applications. In addition, high-fidelity large-eddy simulations were conducted, both for real storm events and for idealized atmospheric boundary layers, to complement the measurements. The collected datasets form the observational backbone of the BeFORECAST project, supporting data assimilation, model validation, and forecast improvements across the subsequent work packages.

Table of Contents

1 Introduction

The BeFORECAST project addresses the limitation of sparse offshore measurement by conducting an extensive measurement campaign in the Belgian North Sea with a wide range of technologies aimed at capturing high-resolution atmospheric free-stream and wind-farm flow data. These campaigns executed in the context of Work Package 1 have delivered foundational data to the downstream Work Packages in the project, providing the observational backbone for data assimilation, model validation, and forecast improvements. Furthermore, we investigated the suitability, coverage, and reliability of weather radars and 3-dimensional ultrasonic anemometers.

This deliverable provides an overview of all campaigns and analyses executed within the project (except for the drone measurements which are described in a separate deliverable D1.2). More specifically, this deliverable reports on the activities within T1.1 & T1.2 (measurements within the existing Belgian wind farms, i.e. the "Eastern zone"), T1.3 (measurements on the Westhinder platform – MP7 – near the future Princess Elisabeth Zone, PEZ), T1.7 (assessment of suitability and coverage of operational weather radars), and T1.8 (virtual measurement campaigns in high-fidelity simulations). The locations of the physical measurements are illustrated in Figure 1.

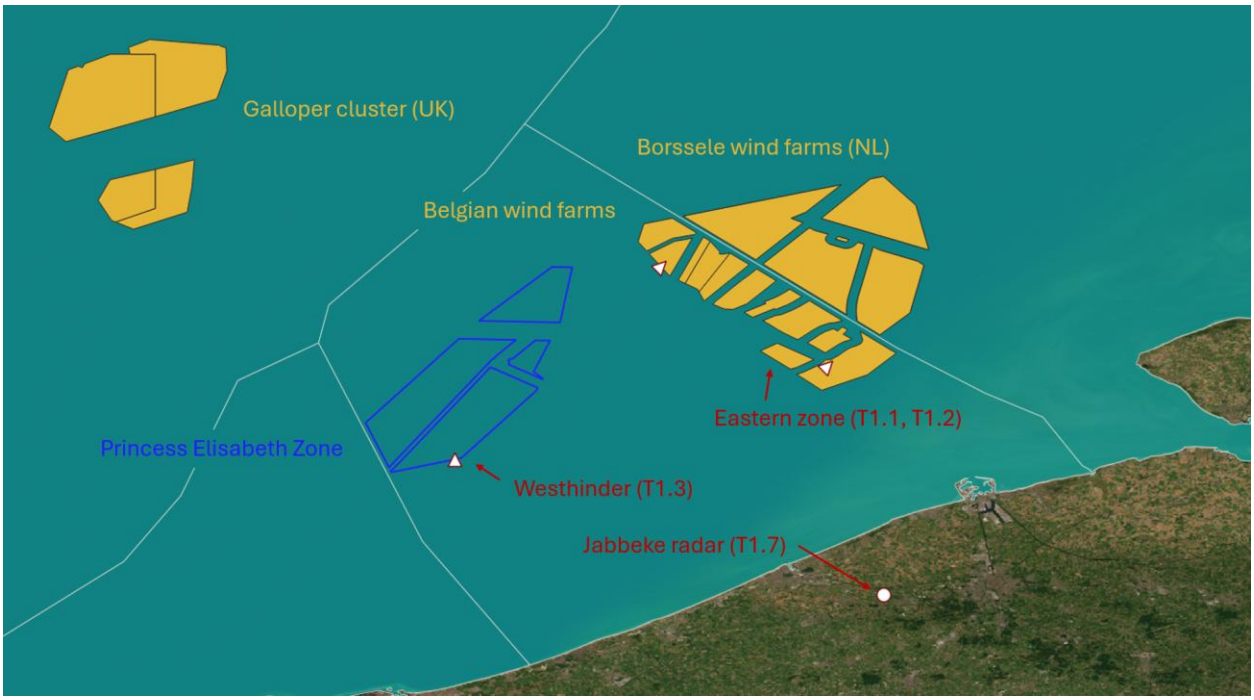

Figure 1: Locations of measurement campaigns in Belgian North Sea. Polygons indicate locations of existing wind farms (yellow) as well as planned Princess Elisabeth Zone (blue).

The remainder of this document is structured as follows. Section 2 elaborates on the LiDAR measurements in the existing zone. Section 3 discusses the campaigns at the southern tip of the PEZ. Next, Section 4 analyzes weather radars in the vicinity of the Belgian North Sea to assess their suitability and coverage for Belgian offshore wind energy applications. Then, Section 5 describes the high-fidelity numerical simulations that were used as an alternative for applications in the project where measurements were missing or impractical. Finally, Section 6 summarizes the main contributions of the BeFORECAST measurement campaigns to the project.

2 LiDAR campaigns in the Eastern Zone (VUB)

In the context of SIM cSBO SeaFD project, ICON Rainbow, and the ETF BeFORECAST project, two nacelle-mounted LiDARs have been installed in the Belgian offshore zone by VUB:

- The Vaisala Wind iris nacelle LiDAR was installed at Norther on 08/2023. The LiDAR was installed on a Norther turbine which is extensively instrumented by VUB within the context of other ongoing research projects (accelerometers, strain gauges, etc.). This instrumentation can help to link inflow conditions and turbine loading. On 05/2024, this LiDAR was moved to Rentel in the scope of an artificial erosion experiment conducted in ICON Rainbow. Relocation of this LiDAR back to Norther is currently being planned in Q4 2025.
- The ZX-TM nacelle LiDAR has been operational within the Northwester2 wind farm since 2022. This LiDAR is facing free-flow conditions along the dominant wind direction in the Belgian offshore zone (South-west), allowing detailed inflow measurements along this direction. The LiDAR has been periodically moved throughout the wind farm in order to gain insights in the accuracy of anemometer measurements at different locations (T2.3). So far, measurements have been acquired at three turbines within the wind farm.

Both LiDARs offer high-resolution line-of-sight measurements and ten-minute wind field reconstructions using internal algorithms. Data from these nacelle-based lidar campaigns is used in the VUB tasks of BeFORECAST, predominantly in WP2.

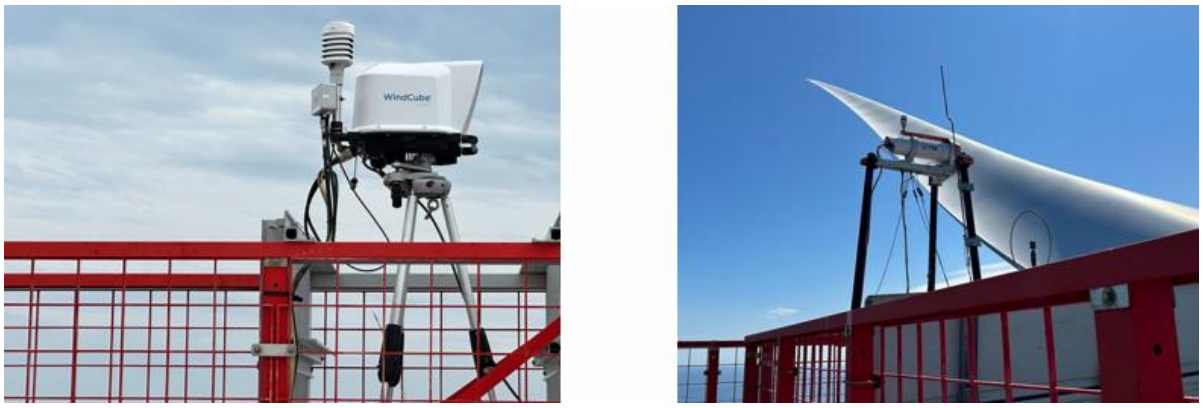

Figure 2: Vaisala Wind iris nacelle LiDAR installed at Norther (Right). ZX-TM Nacelle LiDAR installed at Northwester 2 (Left).

3 LiDAR and ultrasonic anemometer campaigns near the PEZ (VKI)

3.1 VKI Westhinder (MP7) LiDAR

Prior to the BeFORECAST project, in the context of the SIM cSBO SeaFD project, VKI has installed a ZX300M LiDAR on the top deck of the Westhinder survey platform (MP7 – 51° 23.318' N, 2° 26.271' E – see Figure 3). This LiDAR measures at 11 different heights above MSL (32m, 42m, 60m, 77m, 102m, 122m, 147m, 222m, 272m and 322m) at a frequency of 1 Hz per height. A full measurement of the vertical profile therefore takes typically 17s due to the extra time needed for beam focus adjustment and for additional weather condition measurements used in quality control.

The LiDAR was installed in Summer 2021 and gathered data during its first campaign from 04 August 2021 until 18 July 2022, thus providing close to a full year of measurements. In July 2022, it was taken back onshore for necessitated maintenance and upgrades. At the time of writing this document, a second campaign has been measuring continuously since 09 July 2024, thus resulting in a total dataset of over 2 years of measurements. As shown in Figure 4, the data availability after filtering since the first installation of the LiDAR is high during the 2 main measurement campaigns (overall ~97%).

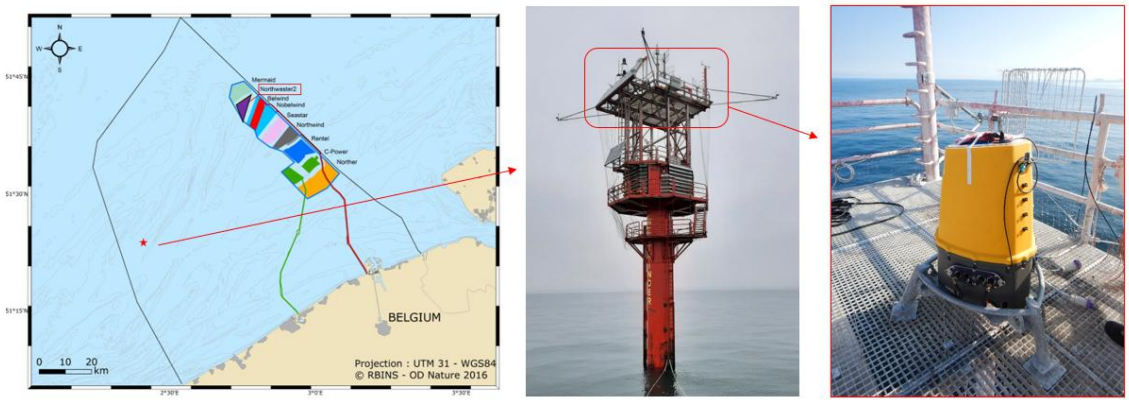

Figure 3: SeaFD ZX300M LiDAR installed at Westhinder (MP7) met mast.

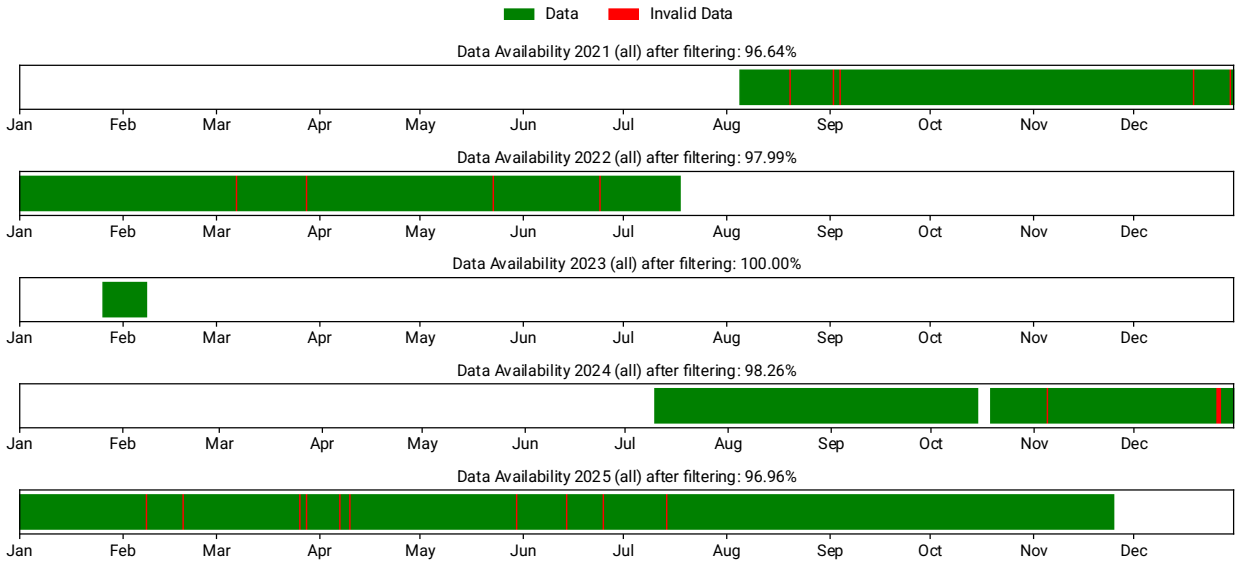

Figure 4: MP7 LiDAR data availability for the different measurement periods at hub height (105m MSL). Colored areas indicate periods of data availability, red areas: data filtered out according to DNV-guidelines. This results in overall data availability after filtering of ~97%.

As a sample of LiDAR outputs, Figure 5 shows seasonally averaged wind roses at 105m above sea level as observed from the LiDAR, highlighting the expected southwesterly dominance in wind directions, and strongest wind speeds occurring during the winter months. Interested parties may access specific segments of this dataset under mutually agreed-upon terms and conditions.

In the context of BeFORECAST, this LiDAR is used predominantly in WP3 (assimilating LiDAR measurements in weather models for improved accuracy), and WP4 and WP5 (for validation of weather models with local freestream measurements).

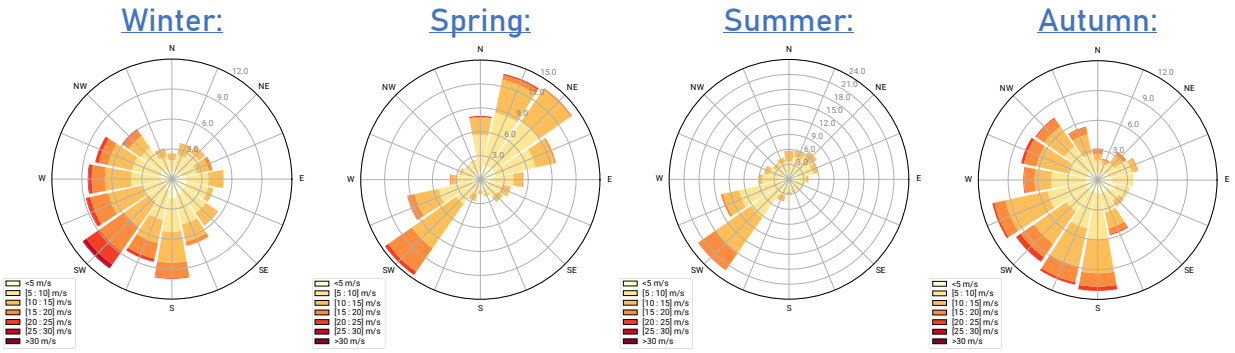

Figure 5: Seasonally averaged wind roses at hub height (105m msl) from Westhinder (MP7) SeaFD LiDAR. Data from Glabeke et al. 2023.

3.2 VKI Westhinder (MP7) three-axis ultrasonic anemometer

In the context of the BeFORECAST project, a three-axis ultrasonic anemometer (3D-USA) has been procured for installation in conjunction with the ZX300M LiDAR at Westhinder (see section 3.1). The primary objective of this initiative is to establish a correlation between the anomalous wind profiles, as determined by the LiDAR, and the atmospheric stability, as calculated by the ultrasonic anemometer.

The 3D-USA model, designated as the Gill HS-100 Horizontal-Head Research Anemometer (see Figure 6), was procured. The horizontal head design ensures that effective measurement of vertical flows is possible, with minimal flow interference from the anemometer geometry. The HS-100 is capable of monitoring wind speeds ranging from 0 to 45m/s while delivering rapid updates at a frequency of 100Hz that enable accurate wind analysis. This is achieved with a resolution of 0.01m/s and an accuracy of less than 1% RMS. It is imperative to note that the accuracy specification is applicable to wind speeds of less than 32m/s and azimuthal angles of less than ±150°, with a tilt angle of up to ±50°.

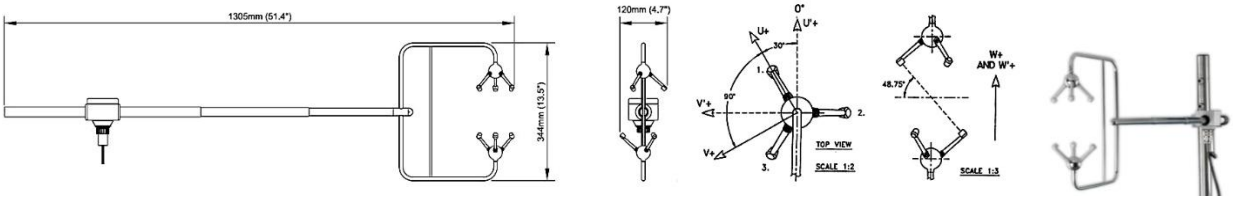

Figure 6: Geometry of the sensor head of the Gill HS-100 Horizontal-Head Research Anemometer with its three upper and lower transducers and the vertical distance between the transducers is about 100mm.

In the initial phase, the 3D-USA was installed in the large open-jet wind tunnel (VKI L-1A) at the von Karman Institute. This was then compared with a reference instrument at varying turbulence levels, as outlined in Glabeke et al. (2024). This investigation was undertaken after a bibliographic study where authors questioned the applicability of wind tunnel calibrations, typically at low turbulence levels, to field conditions. From the conducted tests we could conclude that, under conditions of low turbulence (turbulence intensity of TI less than 1%), the level of precision of the 3D-USA adheres to the manufacturer's specifications. However, certain challenges were observed when exposed to a more

turbulent atmosphere with a turbulence intensity of approximately 6.1%. In this scenario, the HS-100 not only overestimated the measured wind speeds in comparison to the reference probe but also exhibited a systematic shift when compared to the low-turbulence case. The findings demonstrate that the HS-100 is sensitive to turbulence, thus highlighting the necessity for further research into the root cause of this inaccurate behavior.

In a subsequent phase, the 3D-USA system was installed onshore at the test site of the Flemish government agency Vlaamse Hydrografie, under the authority of Maritieme Dienstverlening en Kust (MDK) in the port of Ostend (see Figure 7). The primary objective was to ensure the seamless functionality of the power and measurement chain, which is identical to the configuration employed offshore at MP7.

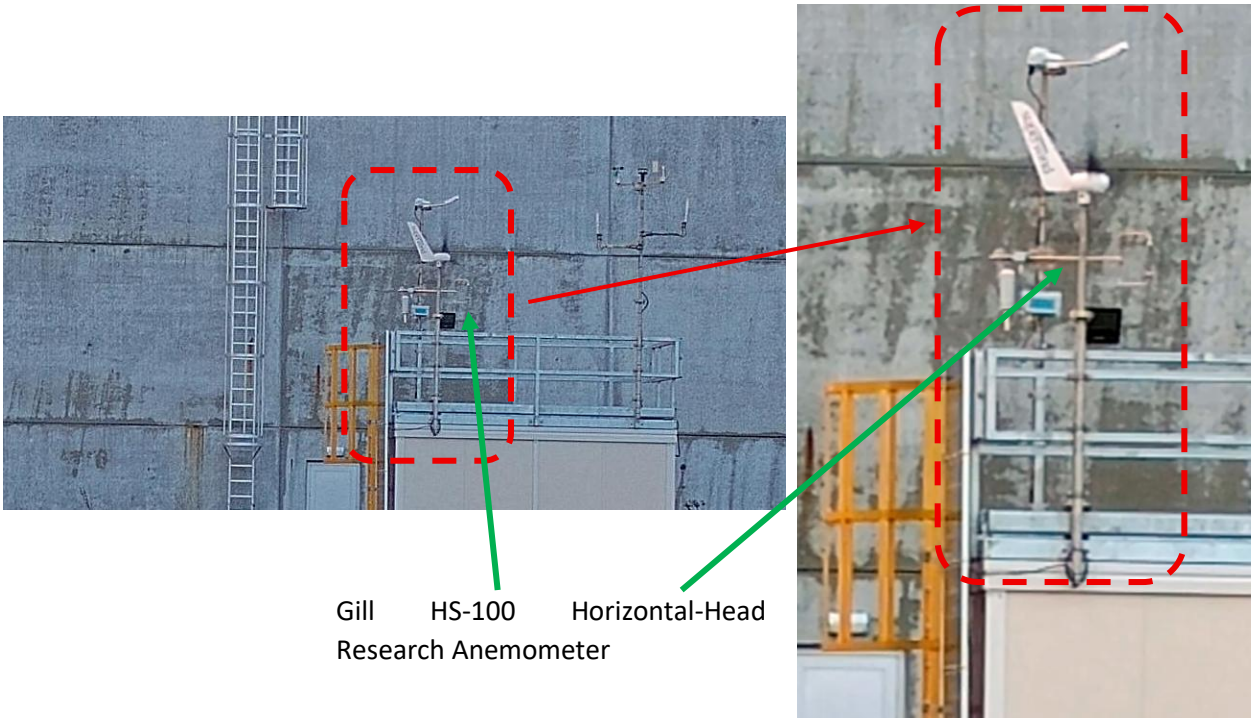

Figure 7: 3D-USA system installed onshore at the test site of the Flemish government agency Vlaamse Hydrografie, under the authority of Maritieme Dienstverlening en Kust (MDK) in the port of Ostend.

Following successful onshore testing, the plan was to transfer the sensor to MP7 and install it above the water on the south-west corner of MP7, where it would provide offshore wind measurements. However, due to power supply issues at MP7, this could not be completed within the timeframe of the current project, so the sensor is still installed onshore at the time of writing this report. However, a major renovation of the MP7 power supply system has recently been completed, resolving previous constraints, and the sensor is now scheduled for installation on MP7 in spring 2026.

4 Assessment of coverage and suitability of weather radars for Belgian wind farms (RMI)

Weather radars play a crucial role in observing and short-term forecasting precipitation patterns and (thunder)storm dynamics. Their working principle is to detect intensity and timing of backscattered radiation from hydrometeors, giving information on intensity and location of precipitation over a typical

range of 100 km from the radar location. Furthermore, modern weather radars are mostly Doppler radars, which can also extract information on the velocity of the hydrometeors and hence on the radial wind field. Within T1.7, the aim is to assess the coverage and suitability of weather radars for detecting and forecasting precipitation and wind conditions for Belgian offshore wind farms. This section provides a summary of the full activities of T1.7, a fully detailed report can be found in Appendix A.

In Belgium, currently 4 weather radars are operational (see Figure 8a), i.e. in Wideumont, Helchteren, Zaventum, and Jabbeke. These radars have a maximum detection range of up to 300 km, with quantitative measurements being limited to about 100 km. As shown in the Figure, this implies that the Jabbeke C-band dual-polarization Doppler LiDAR is of main interest for the Belgian offshore wind farms. Although the remainder of this section will focus on the Jabbeke radar, note that the Belgian North Sea is also in the maximum velocity detection range of several radars from neighboring countries (Figure 8b), more specifically Abbeville and Avesnois in France, and Herwijnen in the Netherlands.

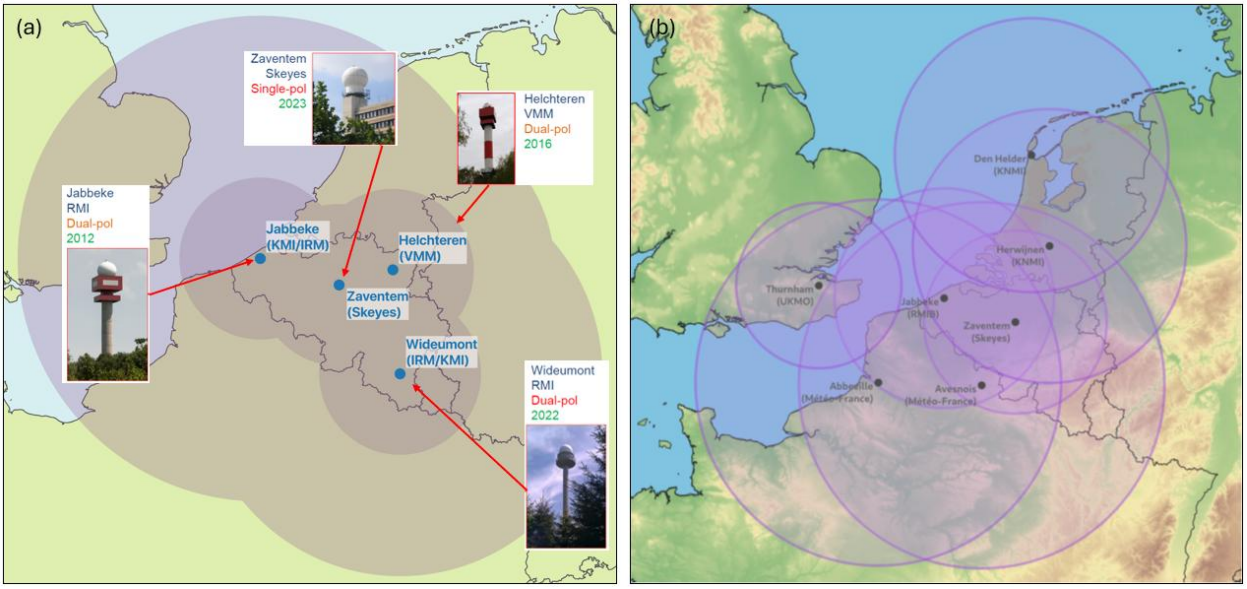

Figure 8: (a) Operational weather radars in Belgium. The maximum combined precipitation detection range is shown in light shading, whereas dark shading indicates the region for which quantitative precipitation observations can be extracted. (b) Operational weather radars in the vicinity of the Belgian North Sea. Shading indicates the maximum detection range for velocity.

We now turn the focus on the Jabbeke radar due to its proximity to the Belgian wind farms. Since its commissioning in 2016, an average availability of the platform of 94.98% is observed, with most recent years all exceeding 96.9%, indicating a very high availability.

To assess the coverage of the radar measurements for the Belgian wind farms, we examine the radar scanning strategy, which consists of an azimuthal scan at different elevation angles to gather information from different heights at different distances. More specifically, its scanning strategy consists of an azimuthal rotation at 15 elevation angles ranging from 25 degrees to 0.3 degrees as shown in Figure 9, where a full scan is completed every 5 minutes. The figure illustrates the centerline height of the radar beam as a function of distance from the radar. As shown, at the location of the Belgian wind farms the velocity measurement ranges from approximately 300 m for nearby wind farms like Norther to 900 m for the furthest farms like Mermaid. This implies that, although the radar scan strategy covers heights in the boundary layer above the wind turbine canopy, hub height measurements cannot be obtained.

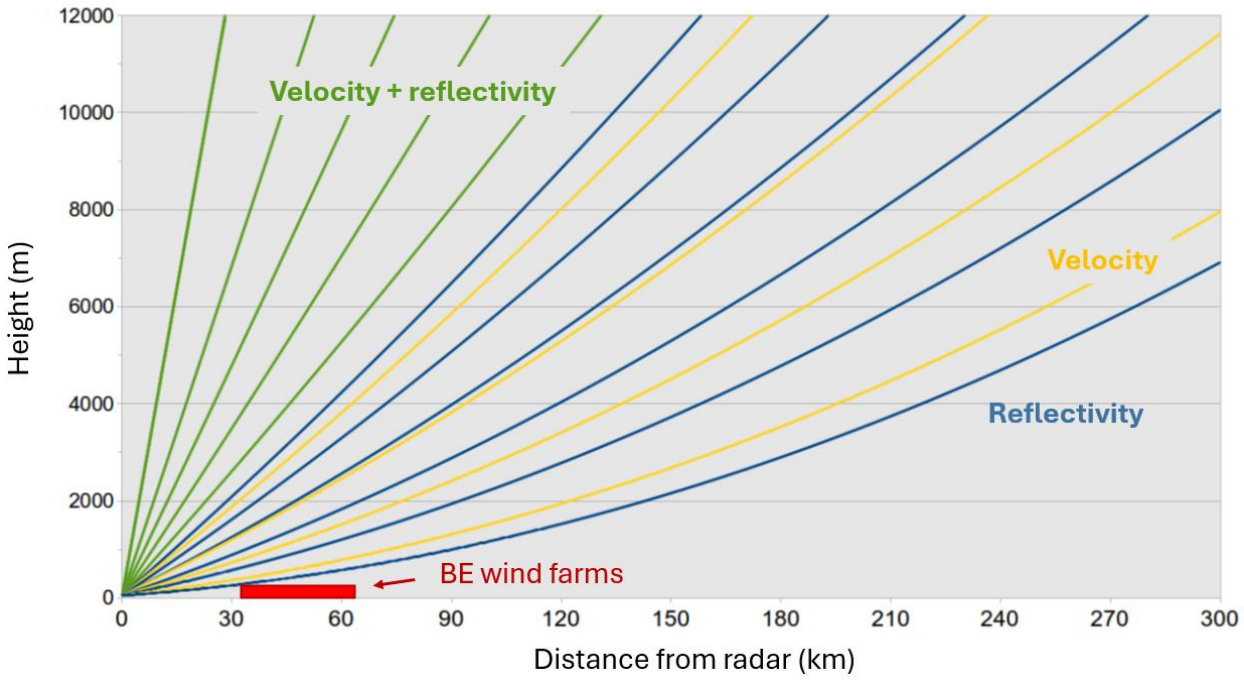

Figure 9: Scanning strategy Jabbeke radar. Blue lines indicate reflectivity measurements, yellow lines indicate velocity measurements. Green lines indicate combined reflectivity and velocity measurements. The approximate location of the Belgian wind farms is indicated in red.

To further assess the suitability of radar measurements for offshore wind farm applications, Figure 10 illustrates some sample outputs from the Jabbeke radar. Figure 10a shows reflectivity measurements from the lowest elevation angle (i.e. for altitudes closest to the wind turbine canopy). A first observation is that the reflectivity measurement is affected by noise from obstructions closeby the radar, as well as a signature of the wind farms. Spurious reflectivities up to 60 dBZ are observed, which would typically be caused by extreme hail. While the former originate from stationary obstructions and can be filtered out with relative ease, the wind farm signatures are much more difficult to filter out due to the rotating blades of the wind turbines, thus significantly impacting any measurements in the close vicinity of the wind farm. Measurements can then be aggregated into a composite image at a specific height by combining data from different elevation angles.

Figure 10b illustrates a typical radial velocity measurement visualization from a Constant Altitude Plan Position Indicator (CAPPI) view at 1 500 m altitude, which is composed from a combination of radial velocity scans at different elevation angles. The figure clearly illustrates the cyclops syndrome, i.e. in which a single radar can only reconstruct radial velocity V_r and not the full horizontal wind V, for which several overlapping radars would be required. Further note that the horizontal resolution of this CAPPI image is 500 meters.

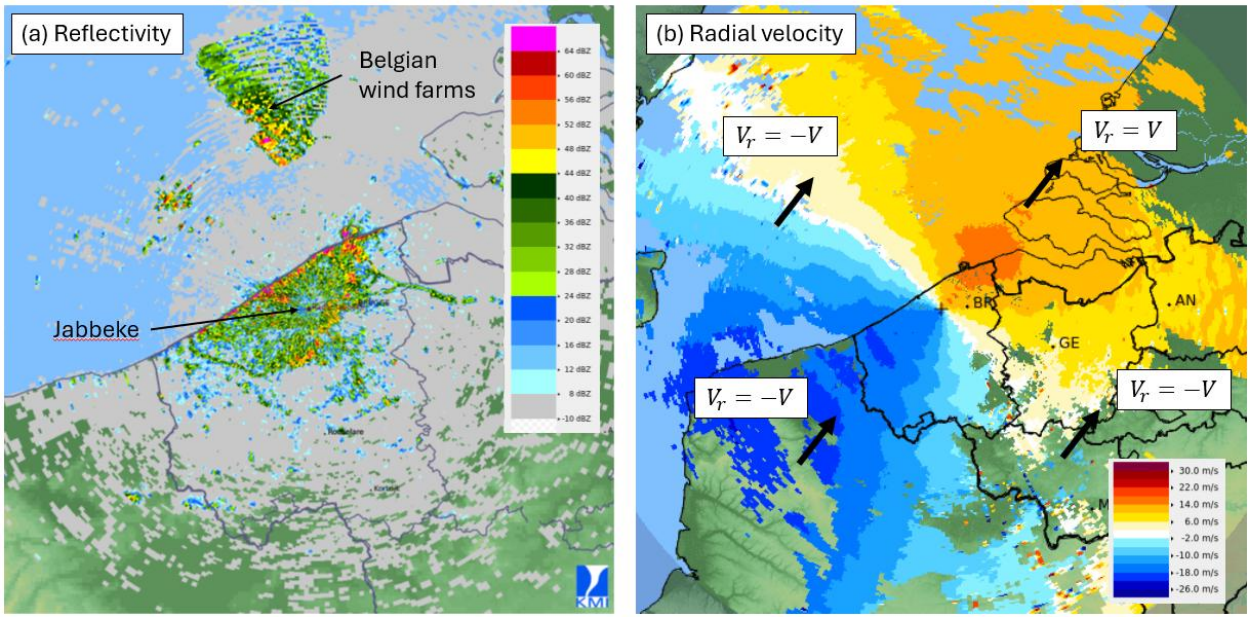

Figure 10: Sample outputs of measurements from Jabbeke radar. (a) Reflectivity measurement at 0.3 degree elevation angle at 12:00:03 on 26 June 2023. (b) Constant Altitude Plan Position Indicator (CAPPI) radial velocity measurement at 1 500 m altitude at 04:15:04 on 2 Aug 2023.

In conclusion, the analysis in the current section highlights the following:

- The Belgian offshore wind farms are within the velocity detection range of 4 radars, i.e. Jabbeke in Belgium, Herwijnen in the Netherlands and Avesnois and Abbeville in France. The Jabbeke radar has a very high availability since its commissioning in 2016.
- The scanning strategy of the closest radar, i.e. the Jabbeke radar, allows for velocity measurements between 300 m and 900 m above mean sea level at the wind farm locations, which is above the wind turbine canopy (up to 200 m tip height for the tallest wind turbines)
- At the lowest elevation height (and thus measurement height) wind turbines significantly pollute the radar signal, impeding accurate measurements in their vicinity. This problem is not present in CAPPI observations at higher altitudes of 1 500 m.

As a result, within BeFORECAST, radar measurements will be used predominantly to improve the accuracy of numerical models for the larger weather scales, i.e. numerical weather prediction models, in the context of WP3 (see D3.1).

5 Virtual measurements in high-fidelity numerical simulations

The original rationale for performing virtual measurements in high-fidelity turbulence-resolving large-eddy simulations (LES) in T1.8 was to provide an alternative source of data in case of issues with the physical measurement campaigns described above. However, these proved not to be blocking for the remainder of the project, so the envisaged simulations were somewhat rescoped compared to the original planning of the project. The first set of simulations described below reproduce 2 high impact weather events in February 2022. The second set of simulations serve as a high-fidelity idealized atmospheric boundary layer flow database for the turbulent flow reconstruction algorithms in WP3.

5.1 Large-Eddy Simulations of Storm events in February 2022 (VKI)

The simulations and results discussed below were presented at an international scientific conference:

- Munters, W., Glabeke, G., Kale, B., Gillyns, E., Buckingham, S., van Beeck, J. Weathering the storm: A large-eddy simulation study of offshore wind flows in transient weather conditions. Presented at the Wind Energy Science Conference, May 2023, Glasgow, UK

During the first Westhinder LiDAR campaign (see Section 3.1), a succession of 3 named winter storms passed over Western Europe in the week of 14 to 21 February 2022, i.e. Storm Dudley, Storm Eunice, and Storm Franklin. High wind speeds during such storm events can significantly impact offshore wind energy, e.g. with significant drops in power output when the cutout wind speed is exceeded. Indeed, as shown in Figure 11, especially during the passings of Storm Eunice and Storm Franklin, significant and sudden power drops are observed, with the former causing a power excursion from full capacity (2.2 GW) to zero in a matter of a few hours.

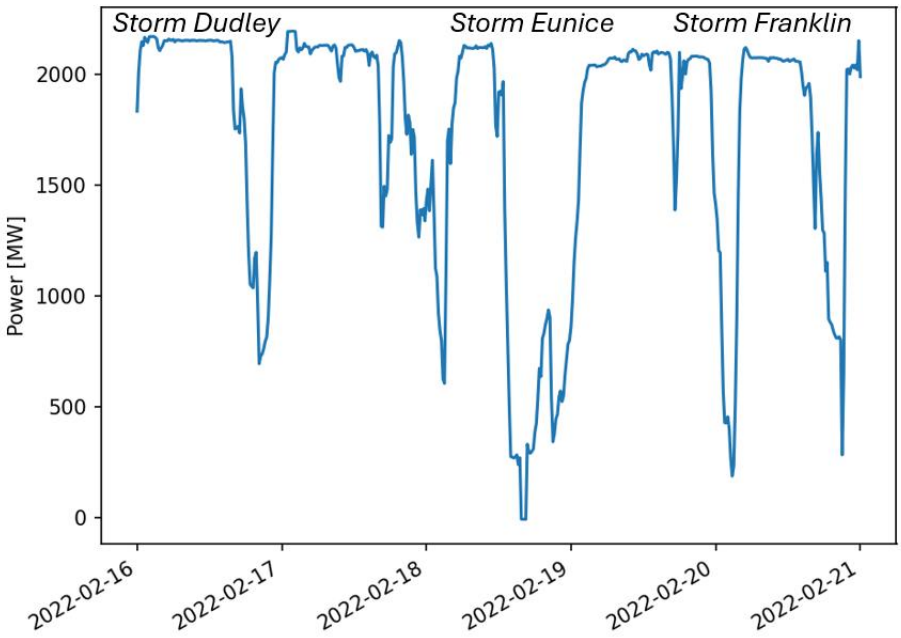

Figure 11: Offshore wind power generation in Belgium from 16 to 21 February 2022. Approximate timings of storm passings are indicated. Data from Elia.

Observing the Westhinder LiDAR measurements in Figure 12, both Eunice and Franklin show some distinct features. Eunice is characterized by an exceptionally high hub height wind speed exceeding cutout wind speed of even the most resilient turbines in the Belgian cluster (i.e. 30 m/s), while the wind direction variation is limited. Franklin on the other hand, while still showing very strong hub height wind speeds between 20 m/s and 30 m/s, shows a sudden shift in both wind speed and wind direction, indicating a frontal passage likely associated with heavy precipitation resulting in missing LiDAR data for a specific time window during the event.

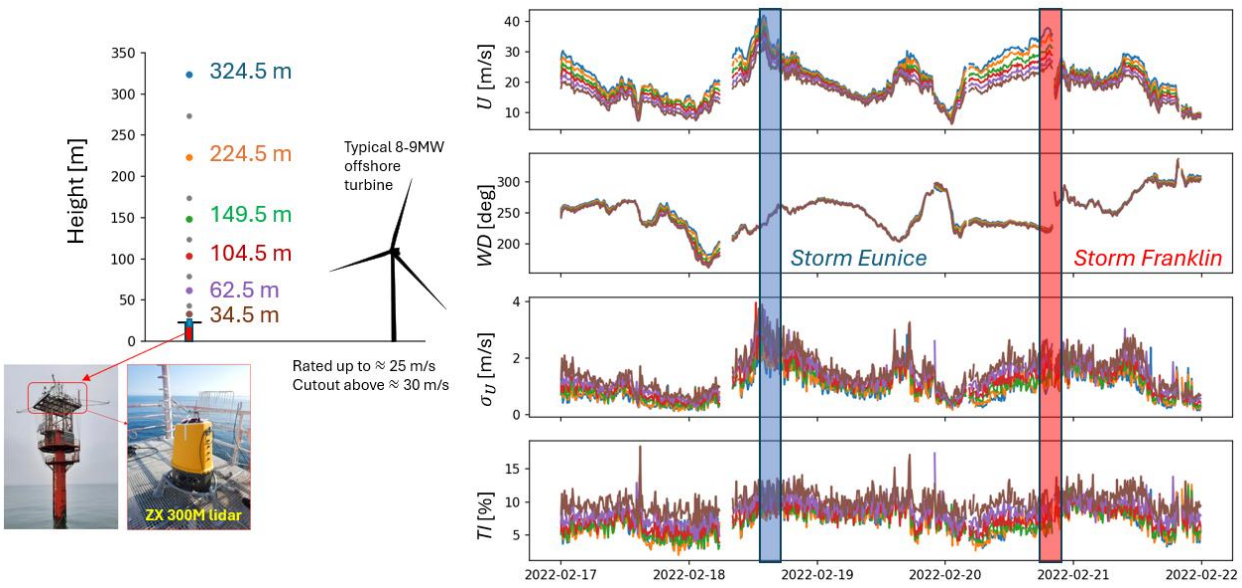

Figure 12: Lidar observations during Storm Eunice and Storm Franklin in February 2022. Specific storm events are highlighted.

As shown above, events such as Eunice and Franklin can have a significant impact on offshore wind farms. Therefore, precise predicting and understanding the atmospheric conditions during such events is of high importance. This motivates the efforts presented here to simulate these events with a multi-scale weather modeling setup down to very high resolutions in the order of tens of meters. To do so, we utilize the Weather Research & Forecasting (WRF) model in a nested domain setup as shown in Figure 13, in which 5 domains are nested inside each other, enabling to increase resolution gradually from 9 km (d01, at the continental European scale with domain extents in the order of 2 000 km) to 72 m (d04, with a limited domain size of 36 km). This procedure allows to both capture the large mesoscale weather dynamics and the detailed local turbulent flow characteristics in the specific zone of interest, in this case the Westhinder LiDAR location. For illustration purposes, also a further refined d05 domain with 24 m resolution is shown in which turbines and their wakes could potentially be included, but these are further not discussed here. Details on the simulation setup can be found in the presentation of Munters et al. (2023), which is added to this document as an appendix.

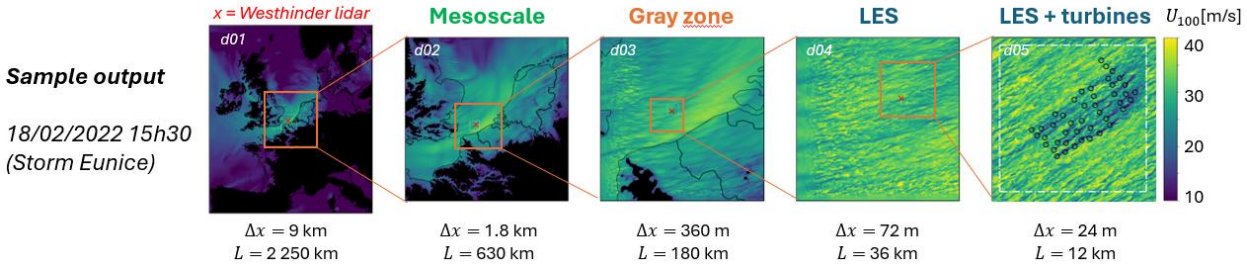

Figure 13: Sample output during storm Eunice illustrating domain nesting setup. In the current report, only results down to d04 (LES without turbines) are discussed.

To assess model sensitivity to turbulence parameterizations, a set of 3 simulations is performed for both Storm Eunice and Storm Franklin. At the Westhinder location (red cross in Figure 13), virtual LiDAR measurements in the form of 10-min averages of wind speed, wind direction, and wind speed standard

deviation are extracted and compared to the LiDAR observation in Figure 14. The figure shows that, for Storm Eunice, the transients in wind speed and wind direction are well captured. Furthermore, wind speed standard deviation is reasonably captured as well. For Storm Franklin however, larger discrepancies are observed. First, the sudden drop in wind speed around 20:30 in the LiDAR observations is not reproduced by any of the numerical simulations. Second, although a 60-degree shift in the wind direction is found in both the LiDAR and the simulations, the latter is lagging the former by approximately 1 hour.

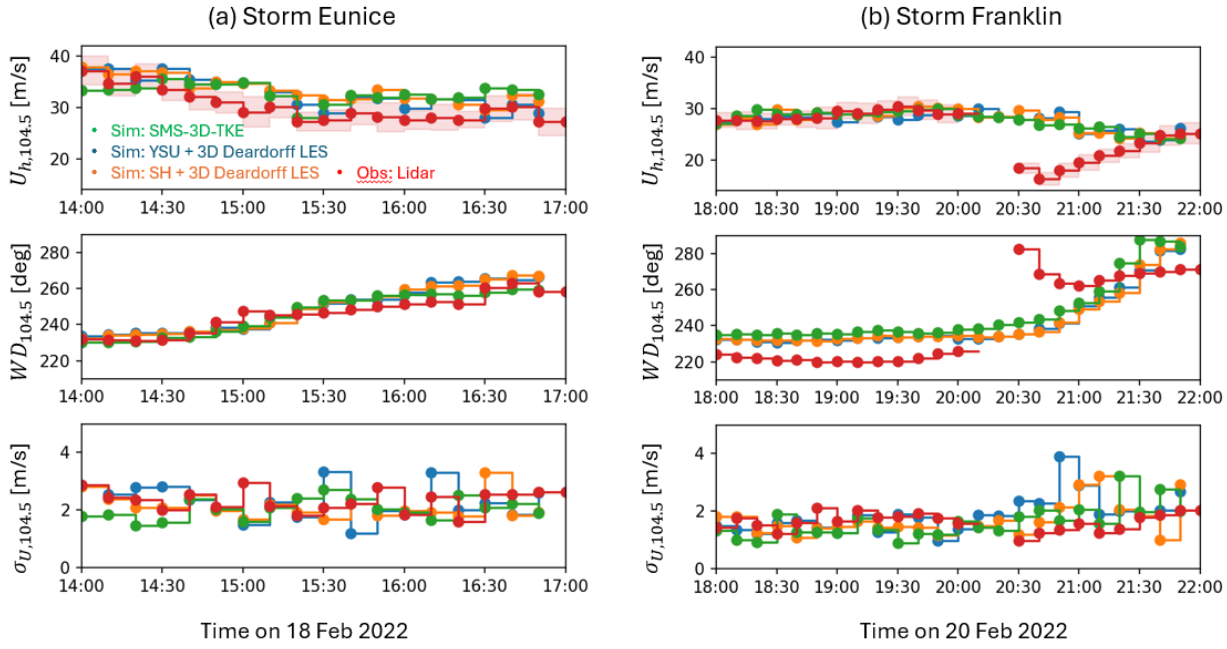

Figure 14: Comparison of simulation results from different setups (green, blue, orange) against LiDAR measurements (red). (Left, a): Storm Eunice. (Right, b): Storm Franklin. Top: Hub height 10-min average wind speed. Middle: Hub height 10-min average wind direction. Bottom: Hub-height wind speed standard deviation.

In conclusion, from the good agreement with the Storm Eunice observations, it is found that multi-scale weather models down to large-eddy simulation scales have the potential to capture high impact weather events, providing valuable insights into atmospheric boundary layer conditions as a complement to sparse observations from LiDARs. However, the Storm Franklin case shows that also key features of such events can appear time-lagged in the simulation results (i.e. the wind direction shift) or not captured at all (i.e. the drop in wind speed). This stresses the need for critical evaluation of numerical models even at very high spatial resolutions.

5.2 Large-Eddy Simulations of idealized atmospheric boundary layers (KU Leuven)

To provide reference data under controlled conditions for the turbulent flow reconstruction techniques of WP3, a set of atmospheric boundary layer LES have been performed during steady, idealized forcing conditions, i.e. with a constant driving pressure gradient and a steady wind direction. Simulations are performed using the KU Leuven in-house pseudo-spectral code SP-Wind. Further information on the details of these simulation datasets can be found in the references included in this section. The use of these datasets within the project is further detailed in BeFORECAST Deliverable D3.2 as well as in the related publications of Alreweny, Vandewalle and Meyers (2024a) and Alreweny, Vandewalle and Meyers (2024b).

A first set of idealized simulations involves the LES of a neutrally-stratified atmospheric boundary layer (i.e., without the presence of wind turbines), in which virtual LiDAR measurements are performed to provide reference data for use in T3.3 (Extending LES-based reconstruction methodology based on weakly constrained 4DVar). A pressure-driven boundary layer is assumed with a height of H = 1 km, a friction velocity of u_* = 0.5 m/s and a surface roughness length of z_0 = 0.1 m. A simulation domain of 30 × 5.4 × 1 km in streamwise, spanwise and vertical directions is used, which is discretized with a fine grid of 2000 × 360 × 200 grid points. Virtual LiDAR measurements are performed using the simulated LiDAR implementation of Bauweraerts & Meyers (2021) which is based on the Lockheed Martin WindTracer LiDAR.

A second set of idealized simulations is performed to provide reference data for T3.5 (Development of operational data-assimilation based on TFT hypothesis and wake models). In this simulation, the effects of the wind turbines are included in the LES using an actuator disk model. The considered wind farm is the TotalControl Reference Wind Power Plant (Andersen et al., 2018), which is composed of 32 DTU 10 MW turbines arranged in an 8 x 4 aligned pattern. Inflow conditions are derived from the publicly available dataset of Munters et al. (2019). The simulation domain has an extent of 16 km × 16 km × 1.5 km in streamwise, spanwise, and vertical directions respectively, with a fine simulation grid of 1200 × 1200 × 225 grid points, resulting in grid spacings of 13.3 m and 6.6 m in horizontal and vertical directions. Power and flow measurements are taken for a time window of 600 s, after a 3 600 s initialization period to circumvent any potential startup transients. Figure 15 shows sample outputs from the simulation, with a snapshot of the flow field in Figure 15a from which the wind turbine wakes can be observed, and 1 Hz wind turbine power measurements in Figure 15b.

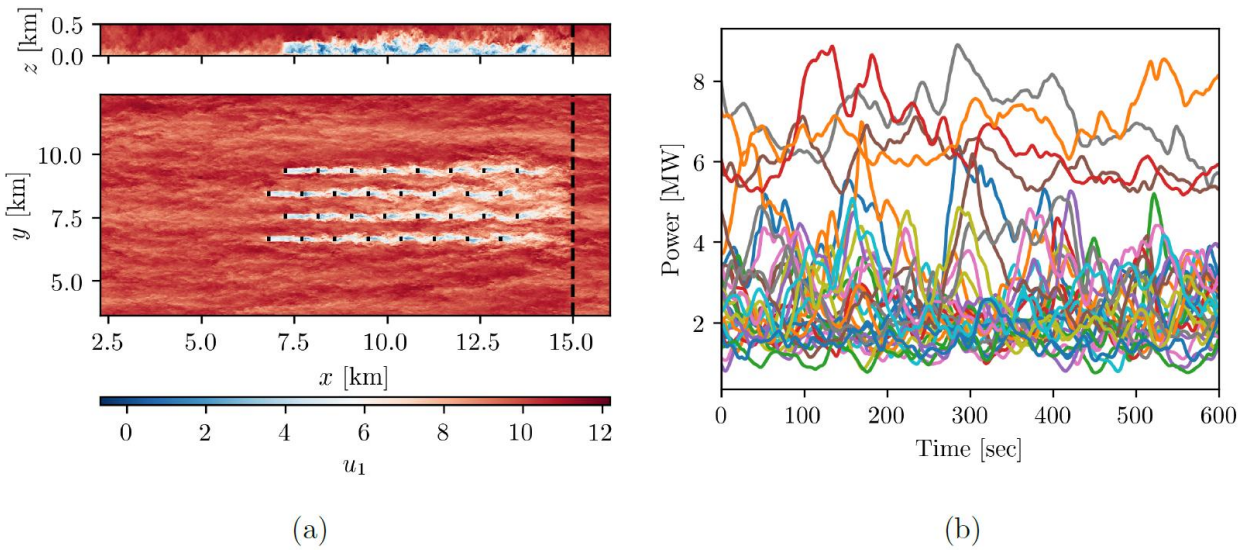

Figure 15: (a) Snapshot of the streamwise velocity of wind farm LES. The vertical dashed line indicates the start of the fringe region. (b) Time series of reference power measurements collected from the wind farm LES. Figure adapted from Alreweny and Meyers, 2024.

6 Summary

The current document described the measurement campaigns conducted in BeFORECAST (except for the airborne drone-based measurements, which are discussed in a separate deliverable). The table below summarizes the main contributions of these campaigns towards implementing tasks in the subsequent work packages

Campaign / dataset	Use in BeFORECAST
T1.1 & T1.2: Wind turbine nacelle-based LiDARs (VUB)	Data analytics, data fusion and machine learning (T2.1, T2.2, T2.3, T2.4, T2.5, T4.1, T5.2, T5.5, T5.6)
T1.3: Westhinder/MP7 campaigns (VKI)	Data assimilation in weather models (T3.2) Weather model validation (T1.8, T4.2, T4.3, T4.4, T5.3)
T1.7: Weather radars (RMI)	Data assimilation in weather models (T3.2)
T1.8: Virtual measurements in high-fidelity simulations (VKI, KU Leuven)	Turbulent flow reconstruction (T3.3, T3.5)

7 Dissemination

The measurement campaigns described in this deliverable support several of the publications of downstream work packages (cf. Section 6). Furthermore, the following dissemination activities are directly linked to the campaigns themselves

- Munters, W., Glabeke, G., Kale, B., Gillyns, E., Buckingham, S., van Beeck, J. Weathering the storm: A large-eddy simulation study of offshore wind flows in transient weather conditions. Presented at the Wind Energy Science Conference, May 2023, Glasgow, UK

- Glabeke, G., Gigon, A., De Mulder, T. and van Beeck, J. How accurate are ultrasonic anemometers, calibrated in a laminar wind tunnel, under turbulent conditions?. Presented at Torque 2024, June 2024, Florence, IT

- Glabeke G, Buckingham S, De Mulder T, van Beeck J. Anomalous wind events over the Belgian North Sea at heights relevant to wind energy. Presented at the Wind Energy Science Conference, May 2023, Glasgow, UK

- Glabeke G., Schena L., Mendez M. A., van Beeck J. and De Mulder T. Observational Study and Probabilistic modeling of Low-Level Jet events happening over the Belgian part of the North Sea. Presented at the Wind Energy Science Conference, June 2025, Nantes, FR

- Ivanova, T., Porchetta, S., Buckingham, S., Glabeke, G., van Beeck, J., & Munters, W. (2025). Improving Wind and Power Predictions via Four-Dimensional Data Assimilation in the WRF Model: Case Study of Storms in February 2022 at Belgian Offshore Wind Farms. Wind Energy Science, 10(1), 245–268. https://doi.org/10.5194/wes-2023-177, https://doi.org/10.5194/wes-10-245-2025

8 References

Alreweny, A., Vandewalle, S. and Meyers, J., 2024a. Large-eddy simulation-based reconstruction of turbulence in a neutral boundary layer using spectral-tensor regularization. *Journal of Fluid Mechanics*, *981*, p.A28.

Alreweny, A., Vandewalle, S. and Meyers, J., 2024b, June. Turbulent flow field reconstruction in wind-farms using power measurements. In *Journal of Physics: Conference Series* (Vol. 2767, No. 9, p. 092032). IOP Publishing.

Andersen S, Madariaga A, Merz K, Meyers J, Munters W and Rodriguez C 2018 TotalControl: Advanced integrated supervisory and wind turbine control for optimal operation of large Wind Power Plants – Reference Wind Power Plant D1.03, Available at: https://www.totalcontrolproject.eu/-/media/sites/totalcontrol/publications/public-deliverables/totalcontrol-d1-03-reference-wind-farm.pdf

Bauweraerts, P. and Meyers, J., 2021. Reconstruction of turbulent flow fields from LiDAR measurements using large-eddy simulation. *Journal of Fluid Mechanics*, *906*, p.A17.

Glabeke G, Buckingham S, De Mulder T, van Beeck J. Anomalous wind events over the Belgian North Sea at heights relevant to wind energy. 2023.Wind Energy Science Conference 2023 Mini-Symposium 1.5 IEA Wind Task 52: Replacing met masts and Accelerating offshore wind deployment. Available at https://doi.org/10.5281/zenodo.8034397

Glabeke, G., Gigon, A., De Mulder, T. and van Beeck, J., 2024, June. How accurate are ultrasonic anemometers, calibrated in a laminar wind tunnel, under turbulent conditions?. In *Journal of Physics: Conference Series* (Vol. 2767, No. 4, p. 042023). IOP Publishing.

Munters W, Sood I and Meyers, J 2019 Precursor dataset PDk, Zenodo [data set], Available at https://doi.org/10.5281/zenodo.2650100

Munters, W., Glabeke, G., Kale, B., Gillyns, E., Buckingham, S. and van Beeck, J, 2023, May. Weathering the storm – A large-eddy simulation study of offshore wind flows in transient weather conditions. Presented at Wind Energy Science Conference 2023, Glasgow, UK, 23 – 25 May 2023.

9 Appendix A: Full detail on Task 1.7 (Radar availability)

Introduction

Several weather radars are installed in the surroundings of the Belgian North Sea Zone. In this report we present the radar measurements with a focus on the data produced by the RMI radar at Jabbeke. It concerns reflectivity data, velocity data, and derived wind profiles. The coverages for reflectivity and velocity measurements of the available radars in Belgium, The Netherlands, UK and France are shown. The impact of wind turbines on weather radar observations is shortly described and illustrated using data from the Jabbeke radar.

Reflectivity measurements

A weather radar is a remote sensing instrument for observing precipitation in the atmosphere. The radar transmits electromagnetic pulses which propagate in the atmosphere. The echoes reflected back to the antenna by the hydrometeors present in the atmosphere allow localizing precipitation and estimating their intensity.

A C-band weather radar operates at 5 GHz. Typical characteristics of a C-band weather radar are gathered in Fig. 2.1. The resolution in elevation and in azimuth is related to the beam width which depends on the antenna size. This size is typically 4 m which gives a beam width of 1 degree. The resolution in range is related to the pulse duration and is typically between 250 m and 500 m. The maximum detection range of C-band weather radar is between 200 km and 300 km. The quality of the measurements tends to decrease with the distance.

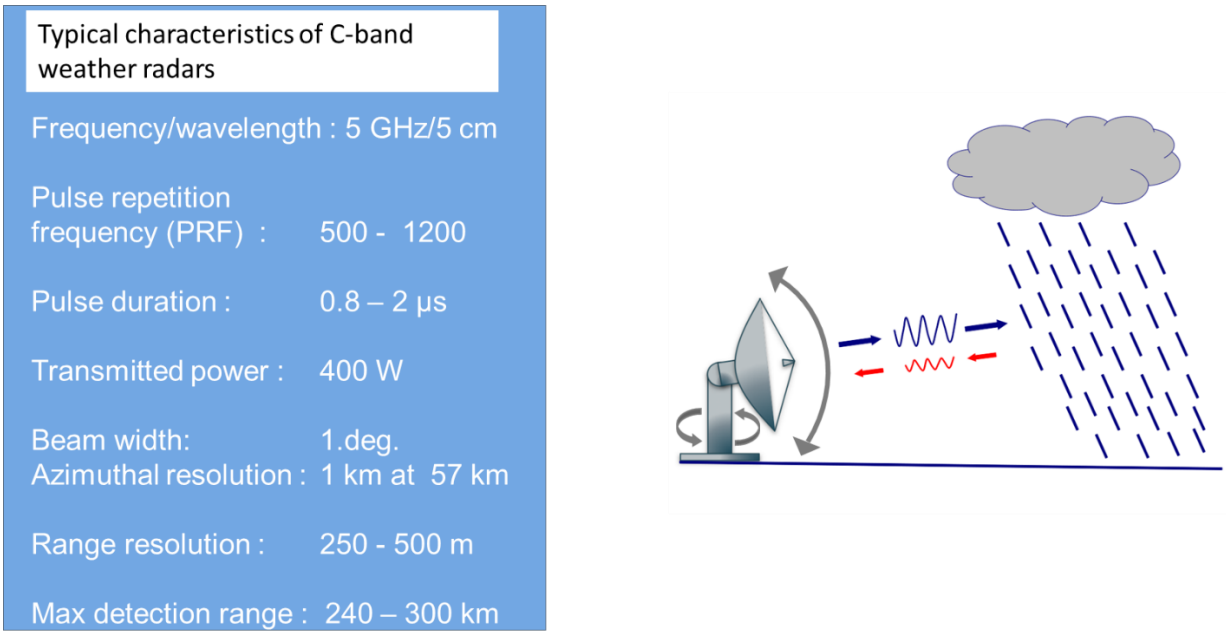

Fig 2.1: typical characteristics of a C-band weather radar

Most radars nowadays perform a volume scan every 5 minutes. Several rotations at different elevation angles are performed during this time interval. Fig. 2.2 and 2.3 shows the scanning geometry and the basic settings of the RMI Jabbeke radar which is the closest radar to the area of interest.

The radar performs 15 rotations between 0.3 and 25 deg. elevation angle. The maximum range for reflectivity measurements is 300 km. The height of the radar measurements increases with the distance. The lowest elevation slice (rotation at a given elevation angle) is close to horizontal but, due to the earth's curvature, the height at 300 km exceeds 6 km.

Some slices are optimized for reflectivity measurements. The Pulse Repetition Frequency for these slices is 500 Hz. Other slices with larger PRFs are optimized for velocity measurements. A dual-PRF (Pulse Repetition Frequency) technique is used to improve the quality of the velocity measurements (see later). For high elevation angles, it is possible to obtain both reflectivity and velocity measurements using high dual-PRF of 1000/800 Hz as will be explained in the next section.

Fig. 2.1: the Jabbeke radar. Installation in 2011.

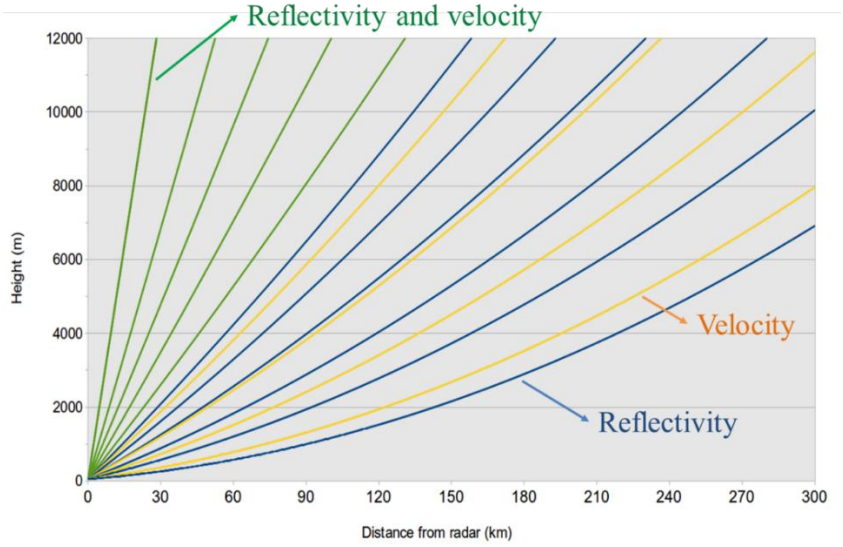

Fig. 2.2: scanning geometry of the Jabbeke radar

	Angle	Measured	PRF	Pulse length	deg/sec
1	0.3	Z, 2-pol	500	2.5	18
2	0.5	V, W, 2-pol	1000/800	0.8	30
3	0.9	Z, 2-pol	500	2.5	18
4	1.2	V, W, 2-pol	1000/800	0.8	30
5	1.5	Z, 2-pol	500	2.5	18
6	2.1	V, W, 2-pol	1000/800	0.8	30
7	2.2	Z, 2-pol	500	2.5	18
8	2.9	Z, 2-pol	500	2.5	18
9	3.4	V, W, 2-pol	1000/800	0.8	30
10	3.8	Z, 2-pol	500	2.5	18
11	4.8	All	1000/800	0.8	30
12	6	All	1000/800	0.8	30
13	8	All	1000/800	0.8	30
14	13	All	1000/800	0.8	30
15	25	All	1000/800	0.8	30

Fig. 2.3: settings of the Jabbeke radar

Radial velocity measurements

Weather radars are now all equipped with the Doppler capability. It means that these radars are able to provide radial velocity measurements. These measurements are based on the phase difference between successive pulses emitted by the radar system and returned by the scattering particles present in the atmosphere. A phase shift between successive pulses is caused by the radial velocity component, which is the component along the line-of-sight. Target velocity at right angles to the radar system line-of-sight does not cause any phase shift, which means that the tangential component of the wind is not detected by the radar (Fig.1).

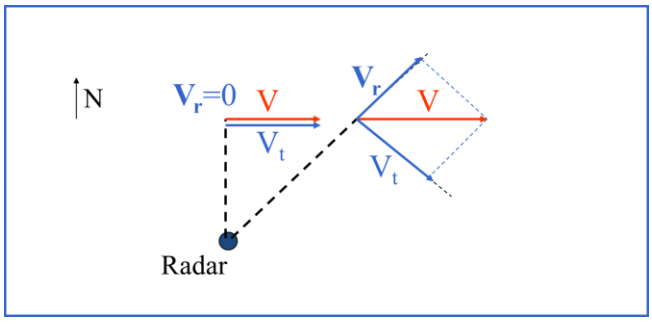

Fig. 2.4: radial and tangential components of the wind vector

It is worth noting that the sensitivity of radar systems for radial velocity measurements is generally higher than for reflectivity measurements. The presence of cloud droplets, dust or pollution particles is generally sufficient to provide a useful Doppler signal. When these targets are moving with the air, the radial velocity is a measurement of the radial component of the wind. Insects also produce a useful signal.

Fig. 2.5 shows an example of a radial velocity product from the Wideumont radar. This image corresponds to a widespread stratiform precipitation field. Negative radial velocities (precipitation approaching the radar) are displayed in blue, while positive radial velocities (precipitation going away from the radar) are displayed in red. The white band indicates radial velocities close to zero. This band, called the zero-isodop line, is perpendicular to the wind direction.

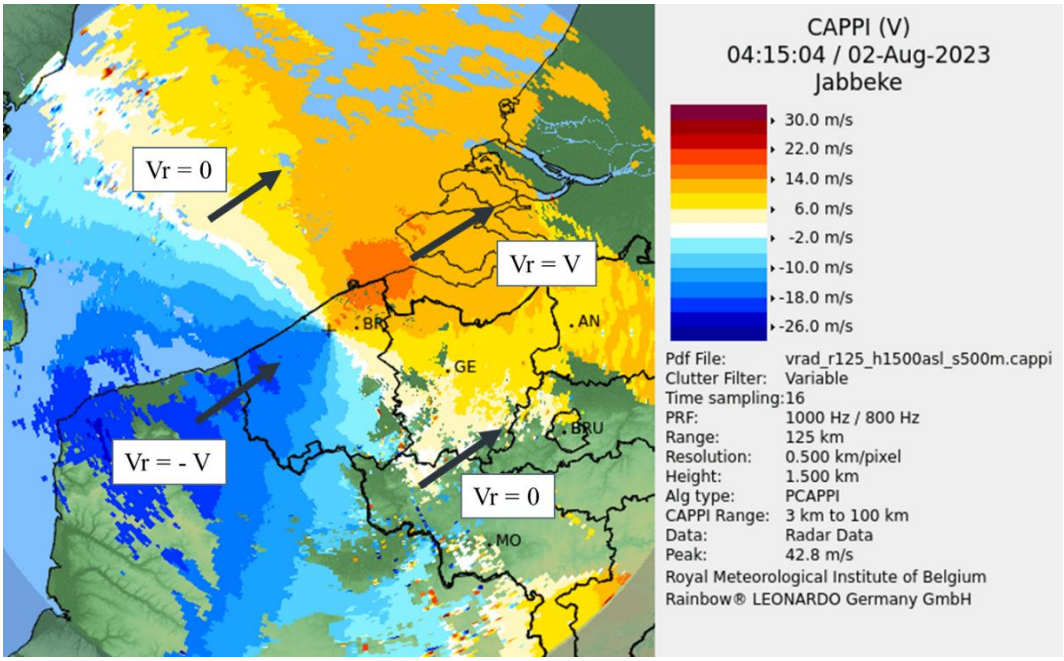

Fig. 2.5: radial velocity product from the Jabbeke radar.

Velocity folding

Velocity detection is wavelength (λ) dependent. As soon as the phase shift between 2 successive pulses exceeds half of the wavelength, the determination of the velocity becomes ambiguous. For a given PRF, the maximum velocity that can be detected without ambiguity is the Nyquist velocity (Vmax = λ PRF / 4). The range of unambiguous measurements is comprised between $-V_{max}$ and $+V_{max}$. Velocity larger than V_{max} or lower than $-V_{max}$ will be folded back into the unambiguous range (Fig. 2.6).

- Maximum unambiguous velocity V_{max}:

$$V_{max} = \frac{\lambda PRF}{4}$$

Pulse to pulse phase shift between – λ/2 and + λ/2

- Maximum unambiguous range R_{max}:

$$R_{max} = \frac{c}{2PRF}$$

- Doppler dilemna

$$R_{max} V_{max} = \frac{c\lambda}{8}$$

For a PRF equal to 500 Hz, V_{max} is equal to 6 m/s. With such a PRF, radial velocity values less than – 6 m/s or larger that 6 m/S will be folded back into the unambiguous velocity interval. For example, a velocity of 8 m/s will be interpreted as a velocity of –4 m/s. A higher V_{max} can be obtained using a higher PRF. However, a too high PRF is not desirable since it limits the maximum unambiguous range of the measurements, which is the longest range to which a transmitted pulse can travel out to and back again between consecutive transmitted pulses.

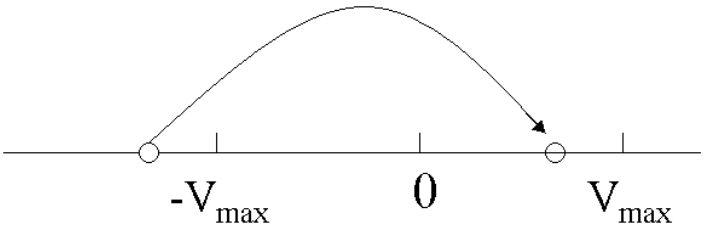

Fig. 2.6: illustration of the velocity folding effect.

Wind profiles from radial velocity measurements

Doppler measurements allow generating vertical profiles of the wind vector around the radar location. In the case of a homogeneous wind field around the radar, the radial velocity at a given height and at a given range, follows a sine function of the azimuth. The phase and the amplitude of this function allow one to retrieve the wind vector as illustrated in Fig. 5. This retrieval can be done at different ranges and for the different elevation angles, which means that a vertical profile of the wind vector can be obtained.

Wind profiles from the Wideumont radar are extracted using a Volume Velocity Processing (VVP) technique. A multi-dimensional and multi-parameter linear fit applied to all available volume data between 5 and 35 km from the radar are used to generate the wind profile. It means that the wind profile is representative of the mean wind in a geographical area between 5 and 35 km from the radar. An example of a wind profile product is given in Fig. 2.7.

Radial velocity measurements require the presence of particles in the atmosphere. As already mentioned, the radar sensitivity for velocity measurements is larger than for reflectivity measurements. Even small particles like cloud droplets, aerosols or dust can be sufficient for producing a useful Doppler signal. It means that the presence of precipitation is not required for producing velocity measurements. Therefore, the availability of velocity measurements and derived products like wind profiles is larger than the availability of reflectivity measurements.

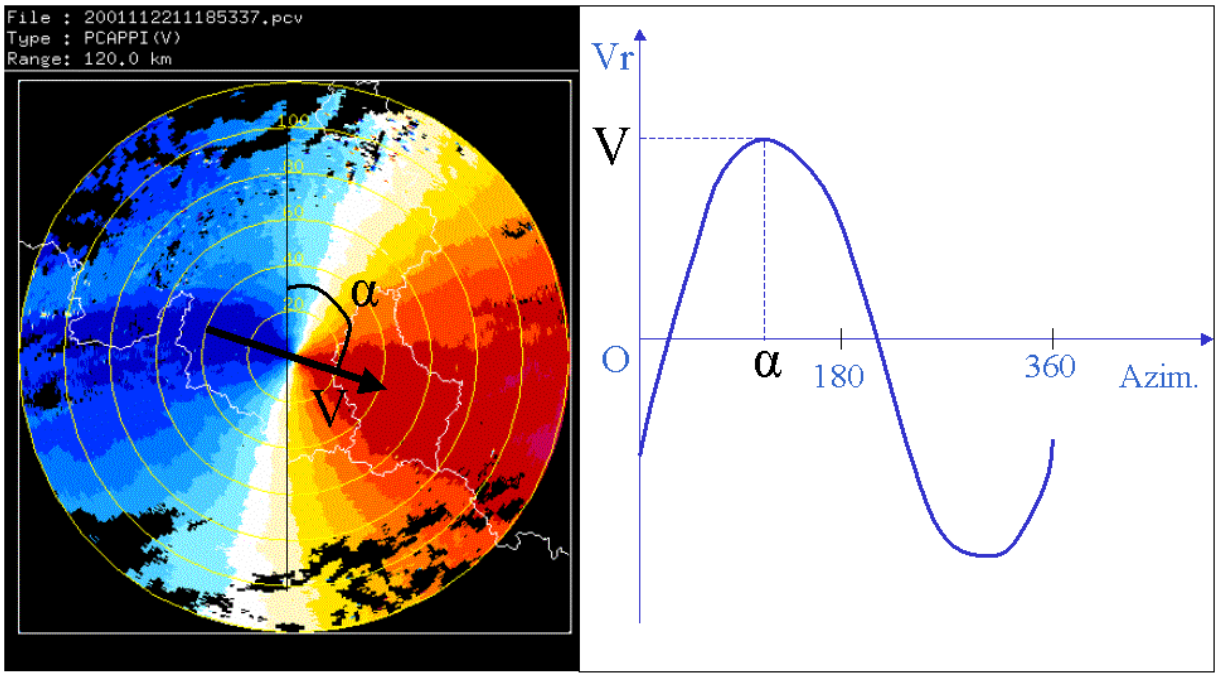

Fig. 2.7: extraction of wind vector from radial velocity measurements.

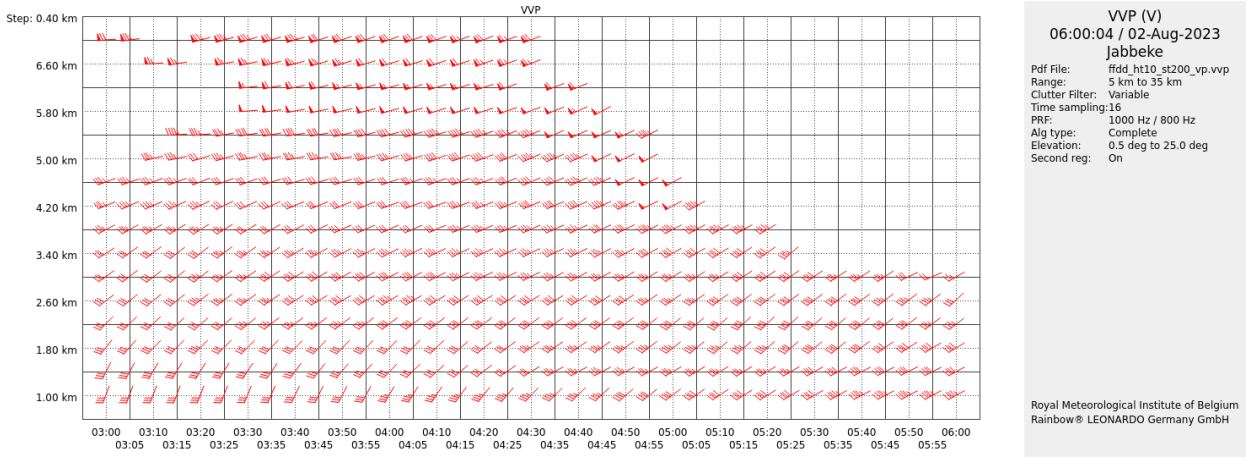

Fig. 2.8: example of wind profile product from the Jabbeke radar.

Radar coverage of the area of interest

The Jabbeke radar is the best located radar for observations in the Belgian North Sea Zone but other radars are also covering the area. As explained in section 2, the effective range for velocity measurements is generally smaller than for reflectivity measurements. Several radars produce reflectivity measurements over the area of interest but no velocity measurements. Table 3.1 lists the available radars, their location and their maximum range for reflectivity and velocity measurements. Fig. 3.1 and 3.2 show the radar coverages for reflectivity and velocity measurements, respectively. The Météo-France radars make use of a specific technique allowing to measure velocity and reflectivity with the same maximum range. For example, the radar of Abbeville produces velocity measurements up to 250 km, which includes the area

of interest. Nevertheless, at such distance the measurements are collected high in the atmosphere and their quality is reduced.

All the available radars, except the Zaventem radar, are dual-polarization radars. These radars produce polarimetric measurements with the same maximum range as for the reflectivity measurements.

Radar	Operator	Latitude (°)	Longitude (°)	Max range Reflectivity	Max range Velocity
Jabbeke	RMI – Belgium	51.1919	3.0641	300 km	150 km
Zaventem	Skeyes-Belgium	50.9054	4.4579	240 km	125 km
Abbeville	Météo-France	50.136	1.8347	250 km	250 km
Avesnois	Météo-France	50.1283	3.8118	250 km	250 km
Herwijnen	KNMI – Netherlands	51.8371	5.138	320 km	187 km
Den Helder	KNMI – Netherlands	52.9528	4.79061	320 km	187 km
Thurnham	UKMO - UK	51.2948	0.6043	255 km	113 km

Table 3.1: weather radars covering the area of interest.

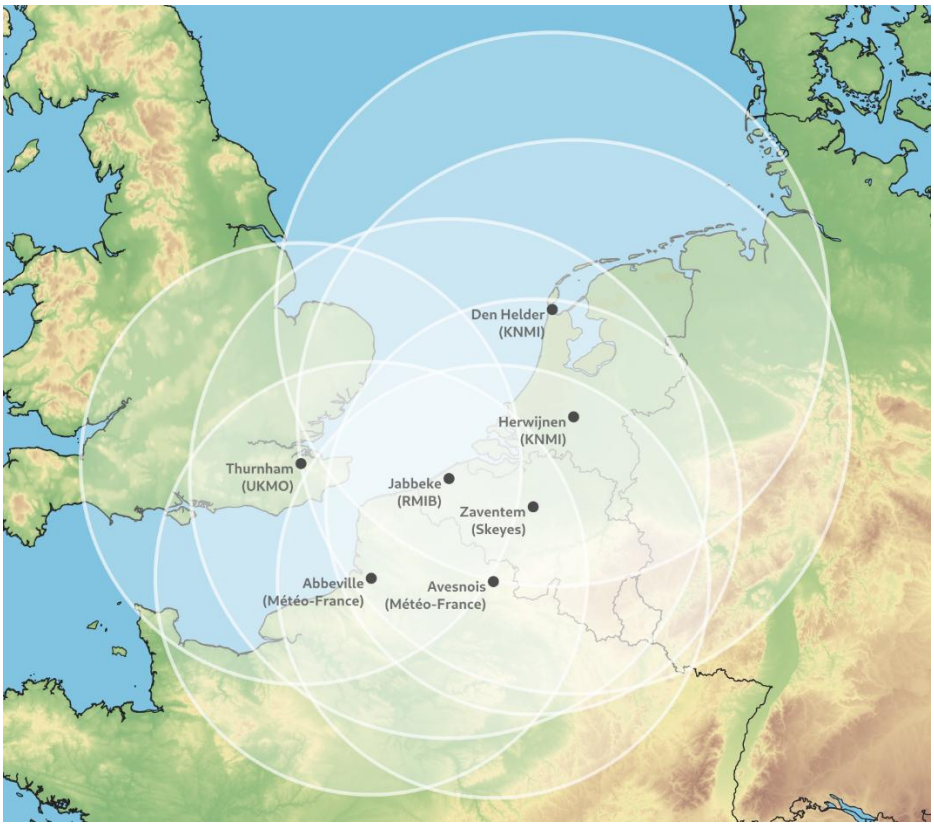

Fig. 3.1: maximum ranges for reflectivity measurements

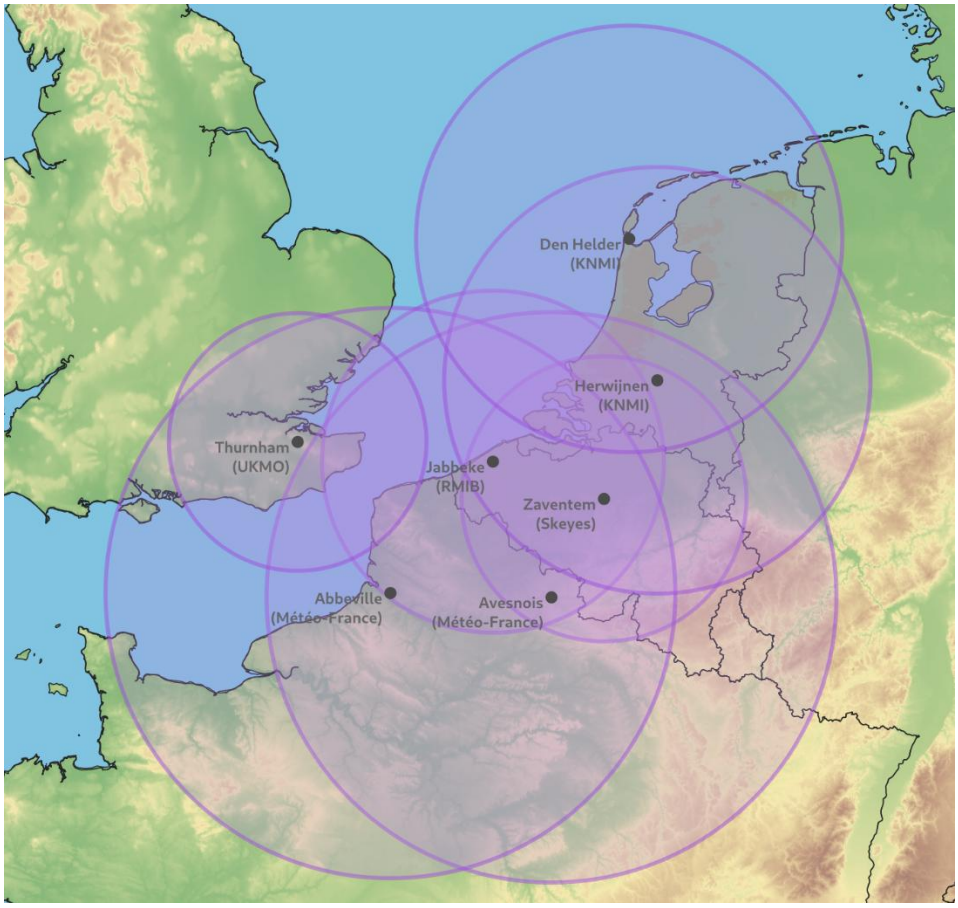

Fig. 3.2: maximum ranges for velocity measurements

All the radars are operational radars functioning 24/7. Maintenance interventions and unexpected failures reduce the effective time of operation but the availability rates of these radars are generally larger than 95 %. Table 3.2 shows the annual availability rates for the Jabbeke radar.

YEAR	Availability (%)
2016	95.57
2017	81.10
2018	95.21
2019	98.56
2020	99.55
2021	96.95
2022	97.97

Table 3.2: availability of the Jabbeke radar data

Impact of wind turbines on weather radar measurements

Wind turbines in the vicinity of weather radars disturb the measurements. The impact of wind turbines on weather radar operations is extensively described in a Eumetnet/OPERA report (Leijnse et al. 2021). When the wind turbine is located in the main beam of the radar, it will partially block the radar beam causing a decrease in the returned power and the derived reflectivity produced by targets behind the wind turbine. Wind turbines also reflect power back to the radar. Because wind turbines are generally constructed of materials that reflect radio waves very efficiently, these reactions can be very intense and visible far from the radar. Besides, the rotating blades of the wind turbines disturb the Doppler signal. Due to the rotation of the blades, the Doppler-based ground echo filtering shows reduced efficiency since this technique assumes that the echoes produced by the ground or fixed objects are stationary.

Fig.4.1 shows the reflectivity from the Jabbeke radar at the lowest elevation angle (0.3 deg.) without any filtering. At short range from the radar, parasitical echoes are produced by various structures at ground level. In the North Sea, radar echoes are produced by the wind farms. In several locations, reflectivity values close to 60 dBZ are observed in this area, which are typical values produced by extreme hail. In the whole area covered by wind turbines the observed reflectivity exceeds 30 dBZ, which corresponds to rain rates exceeding 2 mm/h.

Fig. 4.2 shows the impact of the Doppler filtering on these parasitical echoes. The filtering is much more efficient for removing ground clutter near the radar than for removing echoes produced by the wind turbines. Wind turbines are less visible at higher elevation angles but, as illustrated in Fig. 4.3, the Jabbeke radar measurements at 0.9 elevation angles remain strongly affected.

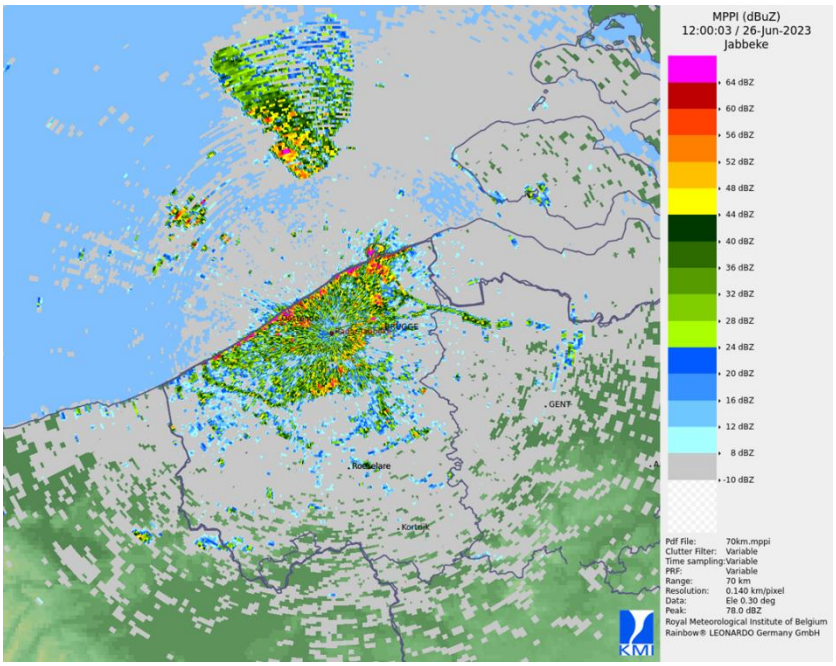

Fig. 4.1: Reflectivity from the Jabbeke radar along the lowest beam at 0.3 deg. elevation without Doppler filtering.

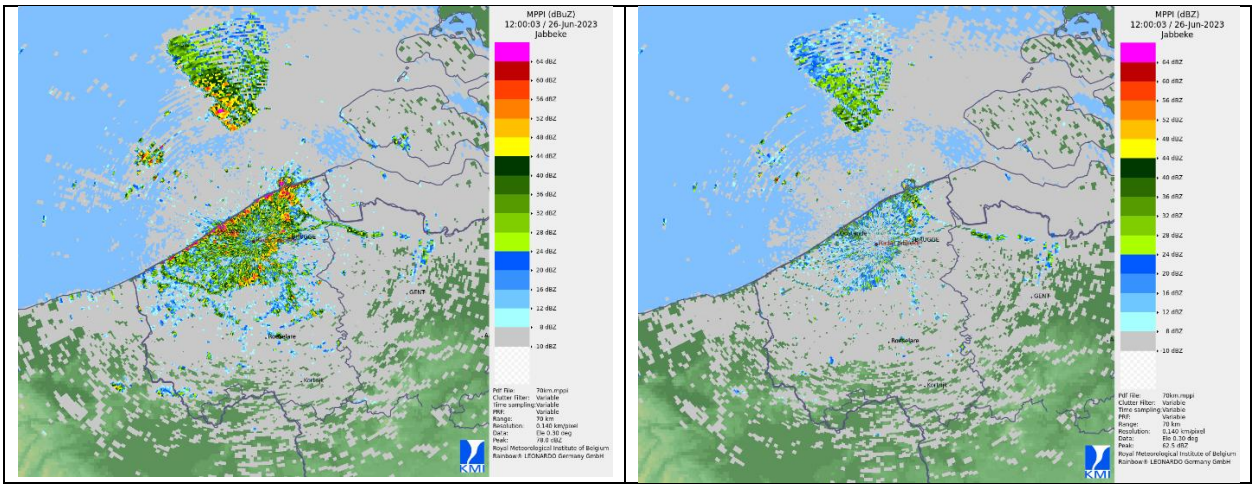

Fig. 4.2: Reflectivity from the Jabbeke radar along the lowest beam at 0.3 deg. elevation without (left) and with (right) Doppler filtering.

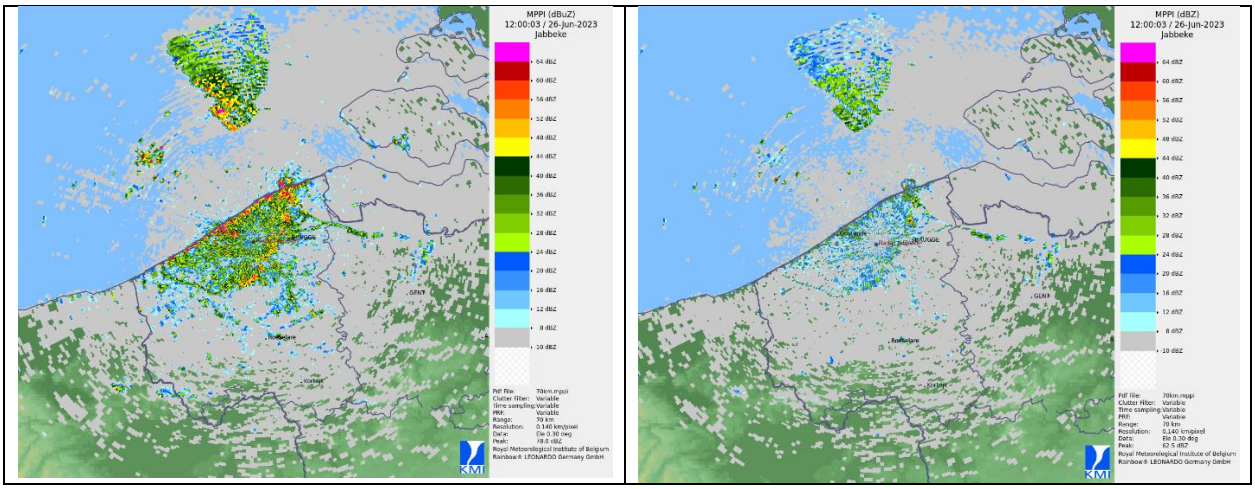

Fig. 4.3: Unfiltered reflectivity from the Jabbeke radar at 0.3 deg. elevation (left) and 0.9 deg. (right).

Conclusion

The area of interest for the BeFORECAST project is well covered by weather radars. The best located radar is the RMI radar at Jabbeke. This radar fully covers the area with both reflectivity and velocity measurements. The Jabbeke radar also produces wind profiles representative of atmospheric conditions between 5 and 35 km from the radar. Several other radars fully cover the area for reflectivity measurements. The radar coverage for velocity measurements is generally smaller than for reflectivity. Consequently, fewer radars are available for velocity measurements. Next to the Jabbeke radar, the KNMI radar at Herwijnen also provides a very good coverage for velocity. All the radars surrounding the area are dual-polarization radars except the Zaventem radar operated by Skeyes.

Weather radars produce valuable observations of precipitation and velocity in the wind turbines zone of the Belgian North Sea. However, it must be kept in mind that the presence of wind turbines disturbs the reflectivity and velocity measurements even at long distance from the radar. Wind turbines produce radar echoes that can be confused with precipitation echoes and a partial shielding of the area behind the wind turbines. Rotating blades disturb the velocity measurements. The disturbances mainly concern the lowest

elevation beams which intercept the wind turbines. Contamination at higher elevations is much more limited. The cohabitation between wind turbines and weather radars is an issue that radar operators and wind turbine promoters have been facing for many years. In this context, it must be noted that offshore wind turbines are less harmful than onshore turbines for weather radar applications. Rainfall has much more impact over land than over sea and a reduced quality of radar observations over sea can be better tolerated than over land. Nevertheless, an impact of offshore wind turbines remains when the radar observations are ingested in nowcasting or forecasting systems. Contamination of radar observations by wind turbines must be properly addressed when using the data for such applications.